INTERNATIONAL JOURNAL OF CLIMATOLOGY
Int. J. Climatol. (2016)
Published online in Wiley Online Library
(wileyonlinelibrary.com) DOI: 10.1002/joc.4586

RMetS
Royal Meteorological Society

Precipitation recycling and soil–precipitation interaction across the arid and semi-arid regions of China

Lijuan Hua,[a] Linhao Zhong[b]* and Zongjian Ke[c]

[a] *Key Laboratory of Computational Geodynamics, University of Chinese Academy of Sciences, Beijing, China*
[b] *Key Laboratory of Regional Climate-Environment for East Asia (RCE-TEA), Institute of Atmospheric Physics, Chinese Academy of Sciences, Beijing, China*
[c] *Laboratory for Climate Studies, National Climate Center, China Meteorological Administration, Beijing, China*

ABSTRACT: Dynamic recycling model (DRM) and reanalysis data were used to study the interaction between the land surface and atmosphere during the warm season from 1979 to 2010 across the arid and semi-arid regions of China. The nonlinear trends common to the key land–atmosphere interaction variables were extracted. For the whole study region, the precipitation recycling ratio showed an increasing trend, especially in the period before the 1990s. Simultaneously, increasing trends were also found in variables regionally related to precipitation, such as soil moisture, evaporation, precipitation efficiency, low-level cloud and precipitable water. However, the moisture transport due to westerly moisture flux showed a remarkable weakening throughout the whole study region. Based on significantly positive correlation between the precipitation efficiency and precipitation recycling ratio under relatively low moisture advection, it was concluded that the precipitation recycling process should not been ignored, for both direct and indirect precipitation processes, in the study region. The spatial patterns of nonlinear trends in land–atmosphere interaction variables indicated reverse tendencies in two sub-regions divided by the meridional boundary at approximately 110°E. For the western sub-region, although decreasing westerly moisture flow was found, the strengthening southerly moisture flux mainly resulted in an increase of precipitable water. Positive relationships among precipitable water, low cloud, precipitation, soil moisture, evaporation and the precipitation recycling ratio were also found. The soil becoming wetter and the precipitation recycling process becoming enhanced suggested the existence of positive land–atmosphere interaction in the western sub-region. However, the opposite tendencies were found in the eastern sub-region, where a weakening of advected moisture convergence was caused by decreases in both westerly and southerly moisture transport. Furthermore, less evaporation and warming temperatures suggested the climate in the eastern sub-region shifted towards relatively warmer and drier conditions throughout the course of the study period.

KEY WORDS regional precipitation recycling; soil–precipitation interaction; arid and semi-arid regions; dynamic recycling model

Received 8 January 2015; Revised 5 October 2015; Accepted 5 November 2015

1. Introduction

Land surface–atmosphere interaction plays a crucial role in the global climate, and understanding these interactions will enhance the ability to predict hydrologic variability (Dominguez and Kumar, 2008). Many previous studies have indicated an important role of the land surface in atmospheric conditions at a broad range of time scales, as well as spatial scales (Rowntree and Bolton, 1983; Nicholson, 2000; Koster *et al.*, 2004; Santanello *et al.*, 2009; Seneviratne *et al.*, 2010; Taylor *et al.*, 2011, 2012; Risi *et al.*, 2013). Risi *et al.* (2013) pointed out that land–atmosphere feedbacks are either local or regional. Local feedbacks involve complex land–atmosphere interaction processes, which depend on the effect of surface fluxes on the local atmospheric conditions, large-scale atmospheric conditions, the spatial scale of soil moisture anomalies, and so on. But for regional feedbacks, the related processes involve the effect of surface fluxes on remote atmospheric conditions and large-scale circulation. In addition, regional-scale feedback strongly depends on the climate type, regional area, as well as the method used to quantify it.

The atmospheric water vapour that forms local precipitation in a region is generally divided into two main sources: local evaporation within the region and externally advected moisture (Trenberth, 1999). Precipitation originating from local evaporation is referred to as 'recycled precipitation' (Eltahir and Bras, 1996). Marengo (2006) pointed out that the recycling ratios is a useful diagnostic measure of the interaction between land surface hydrology and the regional climate. Analyses of precipitation recycling have been performed to define the role of land surface–atmosphere interaction and proved to be effective in studying the interaction between the atmosphere or terrestrial variables and precipitation (Eltahir

* Correspondence to: L. H. Zhong, Key Laboratory of Regional Climate-Environment for East Asia (RCE-TEA), Institute of Atmospheric Physics, Chinese Academy of Sciences, Beijing 100029, China.
E-mail: zlh@mail.iap.ac.cn

and Bras, 1996; Trenberth, 1999; Bosilovich and Chern, 2006; Dominguez and Kumar, 2008). Furthermore, studying the links between precipitation recycling and moisture and energy fluxes could also reflect the processes of land–atmosphere interaction (e.g. Brubaker *et al.*, 1993; Trenberth, 1999; Dirmeyer and Brubaker, 2007; Tuinenburg *et al.*, 2011). As a result, identifying the mechanisms involved in the variability of precipitation recycling and its relationships with other physical variables is necessary (Dominguez and Kumar, 2008).

Generally, precipitation, evaporation and remote moisture transport dominate the atmospheric moisture budget equation at the monthly or even longer time scale. Evaporation is closely related to soil moisture, which is a basic land variable affecting the hydrological cycle (Seneviratne *et al.*, 2010). Furthermore, the energy balance partitioning is strongly influenced by soil moisture and is important to the depth of the atmospheric boundary layer (Jones and Brunsell, 2009; Seneviratne *et al.*, 2010), as well as the characteristics of the subsequent precipitation (Brubaker *et al.*, 1993; Trenberth, 1999; Dirmeyer and Brubaker, 2007). Different hypotheses have been presented to describe how soil moisture conditions may affect precipitation occurrence (Alfieri *et al.*, 2008). Generally, soil moisture–precipitation interaction can be summarized as positive feedback (e.g. Eltahir and Pal, 1996; Findell and Eltahir, 1997; Dominguez *et al.*, 2008), negative feedback (e.g. Giorgi *et al.*, 1996; Zangvil *et al.*, 2001; Cook *et al.*, 2006; Dominguez and Kumar, 2008; Hohenegger *et al.*, 2009; Taylor *et al.*, 2011, 2012; Harding and Snyder, 2012a, 2012b; Westra *et al.*, 2012; Bagley *et al.*, 2014) or no feedback (e.g. Salvucci *et al.*, 2002). During the warm season, both positive and negative effects may occur, and a significant feedback can be detected only when one of the two mechanisms is dominant (Alfieri *et al.*, 2008).

The majority of studies support the notion that the strong hydrological coupling of local/regional precipitation and soil moisture over dry land, such as that of northern China, is primarily driven by positive precipitation–soil moisture feedback (e.g. Koster *et al.*, 2004, 2006; Seneviratne *et al.*, 2006; Myoung *et al.*, 2012). However, considering the strong heterogeneity of land cover and its temporal variability, as well as the scarcity of observations, the sign and strength of soil moisture–precipitation interactions remain debated (Seneviratne *et al.*, 2010; Guillod *et al.*, 2014). In fact, a causal relationship between soil moisture and precipitation is very difficult to obtain, even in observations (Teuling *et al.*, 2005; Guillod *et al.*, 2014). Based on the results of a dozen climate-modelling groups, Koster *et al.* (2004) concluded that the evaporation rate was sensitive to soil moisture in dry climates, but to radiation in wet climates. Only in transition zones between wet and dry climates did soil moisture exhibit large variability and evaporation sensitivity to soil moisture, supporting strong soil moisture–climate coupling. That is to say, semi-arid and transition zones are sensitive to climate changes such as potential warming and vegetation variability.

Schär *et al.* (1999) categorized soil moisture and precipitation feedback processes into direct and indirect processes, representative of the processes associated with locally available precipitable water in the atmosphere and those affecting the efficiency of the available atmospheric moisture transforming into precipitation, respectively. The efficiency of precipitation processes through the effects of increasing soil moisture is possibly enhanced by more remote atmospheric moisture entering the region concerned (e.g. Betts *et al.*, 1996; Schär *et al.*, 1999). Because the amount of precipitation partly depends on the evaporation and precipitation efficiency, precipitation recycling is a good indicator for both direct and indirect feedback processes.

China is a vast stretch of land, over which the climate is extremely diverse from region to region. Dry climate generally dominates large sections of western and northern China, occupying more than half of the country, characterized by bare soil and grassland (Chen *et al.*, 2011). The climate of the arid and semi-arid regions of China has experienced rapid change, including an enhanced drying trend in northern China, increased warming, grassland degradation and desertification (Chase *et al.*, 2000; Fu and Wen, 2002; Wang and Zhai, 2003). Previous studies have emphasized that more attention needs to be paid to the arid and semi-arid regions of China with regard to the investigation of land–atmosphere interaction. The response of terrestrial hydrological variables to precipitation and air temperature uncertainty over dry regions is much stronger than over humid regions (Koster *et al.*, 2004; Wang and Zeng, 2011; Liu *et al.*, 2013).

However, reverse wet/dry trends are known to exist in the west and east parts of the arid and semi-arid regions (Wang *et al.*, 2002; Ma and Fu, 2003; Zou *et al.*, 2005). Furthermore, in the warm season (April–September), droughts tend to develop into serious long-term droughts because of rainfall suppression in the dry lands, such as over Mongolia and northern China, where strong hydrological coupling is maintained between regional precipitation and soil moisture (Koster *et al.*, 2006; Wang *et al.*, 2007; Zeng *et al.*, 2010; Myoung *et al.*, 2012).

In the present study, the precipitation recycling process and some hydrological processes in the arid and semi-arid regions across the north of China during the warm season were analysed. Although some studies on the precipitation recycling over northern China, the main Yangtze River basin area, and the middle–lower reaches of the Yangtze River have already been carried (Yi and Tao, 1997; Kang *et al.*, 2005; Fu *et al.*, 2006), a number of problems remain to be solved. First, the process of regional land surface–atmosphere interaction, or the soil moisture–precipitation interaction process in the arid and semi-arid regions of China requires further study. These key problems, if addressed, would help towards a better understanding of land–atmosphere interaction against the current climate background. On the other hand, global warming will have accelerated the hydrological cycle (Brutsaert and Parlange, 1998; Gao *et al.*, 2007). Some studies have indicated a wetting trend appearing in Northwest China, but a similar trend cannot be found in the other northern regions of China (Shi *et al.*, 2003; Ma

and Fu, 2005). Therefore, the second purpose of this study was to identify the differences of land–atmosphere interaction between the west and east parts of northern China. Through analysing the precipitation recycling process, the mechanism resulting in that land moisture difference could potentially be better understood.

2. Data and methodology

2.1. Data

The Japanese 25-year reanalysis (JRA-25) was the main dataset used in this study. JRA-25 is produced using the Japan Meteorological Agency's numerical assimilation system, which employs a three-dimensional variational method and specially collected observational data over the period from 1979 to 2004 (Onogi *et al.*, 2007). After 2004, JMA started real-time operation of JCDAS (JMA Climate Data Assimilation System), and JCDAS inherited the same system as JRA-25. In this study, both products – referred to using the same acronym (JRA-25) and spanning the period 1979–2010 – were used. As the first long-term reanalysis undertaken in Asia, one of the many purposes of JRA-25 is to enhance climatological and meteorological analyses to a high quality in the Asian region. Indeed, many advantages to the JRA-25 reanalysis have been found, such as the predicted 6-hourly global total precipitation distribution and amount being well reproduced both in space and time. Compared to some other reanalysis products, JRA-25 places significant emphasis on the assimilation of data to produce higher quality analyses, particularly in eastern Asia (Onogi *et al.*, 2007). Although hydrological variables have not yet been well investigated in JRA-25 compared with atmospheric variables, some seasonal cycles of hydrological variables, such as soil moisture (especially in the middle latitudes), are well produced because of the high quality representation of precipitation (Nakaegwa, 2008).

The land surface status in JRA-25 is estimated every 6 h by using atmospheric fields during the data assimilation cycle to force the simple biosphere model (SiB). The SiB of Sellers *et al.* (1989) was designed for use in general circulation models of the atmosphere (GCMs) to describe the climatologically important interactions between the terrestrial biosphere and the atmosphere; in particular, the fluxes of radiation, momentum, sensible heat and latent heat (Dorman and Sellers, 1989). The vegetation types obtained from Dorman and Sellers (1989) are used in JRA-25, in which long-term vegetation change is not considered (Onogi *et al.*, 2007). For the analysed region in this work (Figure 1), the main vegetation types were grass, dry area and desert. The grasslands were mainly located in Inner Mongolia, the north of Xinjiang and Gansu, and the dryland areas and desert occupied the rest of the study region. At the simplest level, SiB consists of three sub-models, which describe the processes of radiative transfer (albedo), turbulent transport (roughness length) and the biophysical control of evapotranspiration (surface resistance). Each of these models operates on a set of parameters appropriate to a given vegetation type to

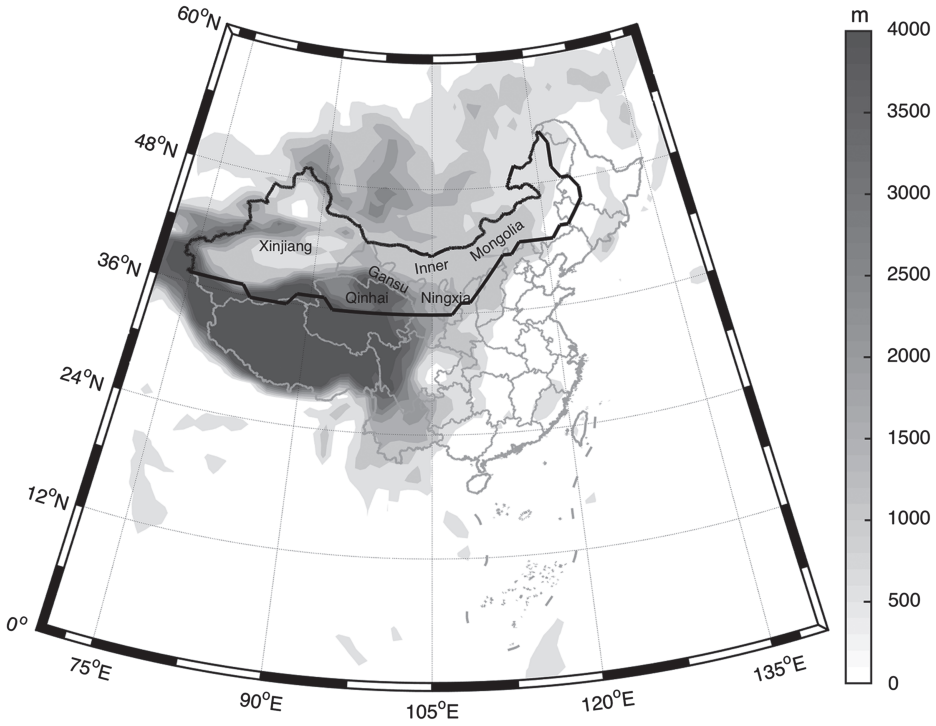

Figure 1. The arid and semi-arid regions of China. The area enclosed by the red line is the analysed region, which mainly includes the provinces of Xinjiang, Inner Mongolia, Gansu and Ningxia, as well as the north of Qinghai Province. The grey lines are the province boundaries. The colouring indicates the height of the topography, as derived from the 2-Minute Gridded Global Relief Data (ETOPO2v2) available at http://www.ngdc.noaa.gov/mgg/global/etopo2.html.

generate the associated properties shown in parentheses. In operation, the full SiB model combines these sub-models to calculate the fluxes of radiation, momentum and sensible and latent heat transfer in a consistent way, with proper regard to the interference of the canopy fluxes on the soil and vice versa (Dorman and Sellers, 1989). In this work, 6-hourly data were produced and a Gaussian-grid subset with a resolution of approximately $1.125° \times 1.125°$ on hybrid sigma-pressure levels was chosen as the basic dataset. The evaporation data were calculated from the latent heat flux at the surface using a constant latent heat of evaporation of $L = 2.507 \times 10^6\,\mathrm{J\,kg^{-1}}$. Owing to strong land–atmosphere interaction occurring more frequently in the warm season, our analysis focused on April–September from 1979 to 2010.

2.2. Precipitation recycling model

Many analytical precipitation recycling models (Brubaker *et al.*, 1993; Eltahir and Bras, 1994, 1996; Schär *et al.*, 1999; Trenberth, 1999; Bosilovich and Schubert, 2001; Gimeno *et al.*, 2012) have been developed based on the work of Budyko and Miller (1974). Dominguez *et al.* (2006) developed a dynamical recycling model (DRM) that included the moisture storage term with the ability to calculate the precipitation recycling ratio at daily scale. Subsequently, this DRM has been widely used to study the precipitation recycling processes across the United States and Europe (Dominguez *et al.*, 2006, 2008; Bisselink and Dolman, 2008, 2009; Dominguez and Kumar, 2008; Harding and Snyder, 2012b). The present study represents a meaningful addition to the literature because the DRM has yet to be extensively applied to the region of China, especially the arid and semi-arid regions in the north.

The well-mixed assumption was used to develop the DRM. This assumption implies that the atmosphere is vertically well-mixed with respect to moisture fractions of different origins, which is one of the simplifications employed in most bulk recycling models (Goessling and Reick, 2011). This assumption limits the temporal scale of the DRM to time scales that are equivalent to boundary layer mixing (Dominguez *et al.*, 2006). The main drawback of this assumption is that locally evaporated moisture tends to locate in the lower atmosphere and less so in the mid and upper levels (Bosilovich, 2003). Burde (2006) emphasized this problem and relaxed the assumption by using an incomplete vertical mixing approach to improve the estimation of 'fast recycling' over the Amazon basin. However, some studies conducted without the requirement of the well-mixed assumption presented similar precipitation recycling ratios as when the assumption was used (Goessling and Reick, 2011). Therefore, considering the complexity of the tracking method in 3-D space, and the 'fast recycling' in the arid and semi-arid region being unlikely to be as effective as in the Amazon, the well-mixed assumption was still used in the present work.

According to the DRM established by Dominguez *et al.* (2006), the start point of model formulation is the full water vapour balance equation. Under the well-mixed assumption, for a given gird cell (i) within the region of concern, the water vapour in the water vapour balance equation can be replaced by the local recycling ratio (ρ_i). In the Lagrangian coordinate, the resulting equation is further transformed into

$$\frac{d\rho_i}{d\mathbf{s}} = \frac{E}{w}\left(1 - \rho_i\right), \tag{1}$$

in which E is evaporation and w is precipitable water. The Lagrangian coordinate variable, $\mathbf{s} = (x - ut, y - vt, t)$, is composed of moisture velocity (u, v), spatial position (x, y) and time t. In fact, $\mathbf{s}$ represents the moving trajectory of the moisture particle, which is the path that links the moisture source and sink. Therefore, ρ_i can be solved directly through integrating the water vapour balance equation in the Lagrangian type along the moisture trajectory. For ρ_i in the grid cell i at time t, the moisture trajectory is produced by tracing back in time, with the start point at the grid cell i and time t, until the trajectory reaches the boundary of the analysed region. In this work, the time-inversing tracing process used the moisture velocity data sampled at daily intervals. After the moisture trajectory became available, through integrating the ratio E/w along the time-inverse trajectory at the daily time scale, the local recycling ratio in grid cell i at time t was obtained as

$$\rho_i\left(\mathbf{s}\right) = 1 - exp\left[-\int_{s_0}^{s} E/w\right] d\mathbf{s}. \tag{2}$$

Furthermore, it was simple to obtain the regional precipitation recycling ratio (ρ_r, hereafter referred to as 'recycling ratio') of the whole region via (Eltahir and Bras, 1994)

$$\rho_r = P_m/P = \sum_{i=1}^{n} \rho_i P_i \Delta A_i \Big/ \sum_{i=1}^{n} P_i \Delta A_i, \tag{3}$$

where P is precipitation, P_m is recycled precipitation and ΔA_i is a grid cell area.

An accurate and reliable moisture trajectory is crucial to obtaining the recycling ratio. In this study, a Lagrangian trajectory tracking method first presented by Blanke and Raynaud (1997), and later developed by Vries and Döös (2001), was used for producing the water vapour trajectory $\mathbf{s}$. This tracking method, having been applied to tracking fluid particle motion in oceanic circulation, directly solves the finite-difference equation of velocity to obtain the analytical (for time-independent cases) and semi-analytical (for time-dependent cases) solutions of the trajectory.

Although recycling ratios estimated by a regional recycling model are influenced by both a region's size and shape (Koster *et al.*, 1986; Eltahir and Bras, 1996; Brubaker *et al.*, 2001; Dominguez *et al.*, 2006; van der Ent *et al.*, 2010), the DRM was still used in this work because the aim of this work was not to identify the origin of the atmospheric moisture over the region concerned, but to investigate the regional hydrological process or the strength of regional land–atmosphere interaction. As such, regional precipitation recycling based on the Largrangian trajectory tracking technique was considered more helpful and directly applicable.

It is very difficult to directly measure signs of land–atmosphere interaction in the real world (Dirmeyer *et al.*, 2009), not only due to the limitations imposed by the available methods, but also the data. In comparison to atmospheric observations, land surface variables such as evaporation and soil moisture are sparsely and rarely observed, but are nevertheless important for analysing the interaction between the land surface and the atmosphere. Recent atmospheric reanalyses have improved remarkably over earlier ones through including the available data, following substantial quality control measures, in a consistent data assimilation system, but all still possess residual problems (Trenberth and Fasullo, 2013). This is another aspect to be dealt with carefully when evaluating the recycling ratio using reanalysis data, of which the physical terms of the reanalysis budgets generally do not balance, even over long periods (Trenberth *et al.*, 2003, 2011; Bosilovich *et al.*, 2011).

In this work, the spatiotemporal average value of the residual term was about $-0.23\,\mathrm{mm\,d^{-1}}$, while the evaporation and precipitation rates were 1.05 and $1.08\,\mathrm{mm\,d^{-1}}$, respectively. A negative value of the residual term may indicate an overestimation of the evaporation term (Draper and Mills, 2008), and does not influence the recycling patterns heavily (Dominguez *et al.*, 2006; Bisselink and Dolman, 2008). Furthermore, the moisture convergence (negative divergence) average of $-0.28\,\mathrm{mm\,d^{-1}}$ was the secondary moisture source in contrast to evaporation, implying that a part of the moisture source for precipitation must come from recycled evaporation (Bisselink and Dolman, 2008). The storage term in atmospheric water is almost negligible, as it is to be expected at long time scales. In short, using JRA-25 reanalysis data to calculate precipitation recycling is useful for studying land surface and atmospheric processes in the present study region.

According to the work of Schär *et al.* (1999) and Asharaf *et al.* (2012), the 'S–P feedback' processes can be divided into direct and indirect processes, with the latter depending on the precipitation efficiency. The regional precipitation variation (ΔP) may be expressed by (Schär *et al.*, 1999; Asharaf *et al.*, 2012)

$$\Delta P = \Delta\chi\left(W_{IN} + E\right) + \chi\left(\Delta W_{IN} + \Delta E\right), \qquad (4)$$

where χ is the precipitation efficiency and W_{IN} is the net inflow of moisture into the analysed region. Precipitation recycling involves both direct and indirect feedback processes because it is part of the water resource for the available water and its transition into precipitation influenced by the precipitation efficiency. Therefore, the precipitation efficiency was also examined in this study to better understand the land–atmosphere interaction process.

2.3. Multi-channel singular-spectrum analysis

To coherently display the variability of the recycling ratio with climate variables, the Multi-channel Singular-Spectrum Analysis (M-SSA) was applied to extract the nonlinear trend signals. M-SSA is the multivariate version of singular spectrum analysis, introduced by Broomhead and King (1986), and is a powerful data-adaptive tool to extract the spatial (multi-variable in this work) and temporal characteristics of trends and nonlinear oscillation embedded in the climate time series. The channels in M-SSA could be the time series of a single variable sampled at different locations in space (e.g. Zhang *et al.*, 1998) or multi-variables sampled in the same spatial location (e.g. Dominguez *et al.*, 2008). In this work, the latter was used to extract the covariation characteristics of the variables within the land–atmosphere system, since this method can decompose the data into modes that capture only the variability common to the entire set of variables (e.g. Dominguez and Kumar, 2008).

The M-SSA is applied to a time series $X(t)$ for L variables (channels), where time $t = 1, 2, 3 \ldots N$. A lagged covariance matrix C of dimensions $(LM \times LM)$ is then constructed, where M is the maximum lag or window of analysis. In essence, the M-SSA is an eigen analysis of the covariance matrix C (Broomhead and King, 1986). The matrix C is diagonalized to obtain LM eigenvalues and LM eigenvectors, not all of them being distinct. The eigenvectors are the channel-time empirical orthogonal functions and the corresponding spatiotemporal principal components are obtained by projecting the original times series $X(t)$ of L channels onto the corresponding empirical orthogonal functions. The part of the original time series that corresponds to a particular eigenmode is extracted by combing its empirical orthogonal functions and principal components to obtain the reconstructed component (RC) (Ghil *et al.*, 2002). The RCs are basically filtered data corresponding to the respective eigenmodes. Furthermore, the RCs have the same variables and the same temporal dimensions as the original time series and capture their phases. The detailed theoretical framework of M-SSA can be found in the works of Broomhead and King (1986), Plaut and Vautard (1994), and Ghil *et al.* (2002).

In the present study, M-SSA was applied to the joint field constructed by the time series of spatially averaged variables listed in Table 1. Each time series represented the regional 32-years (1979–2010) warm-season average of a variable and was standardized to remove the units. The resultant multi-channel (variable) field was inputted into the M-SSA procedure to identify the common signal. In the process of M-SSA, because the window length should

Table 1. Climate variables selected for the M-SSA.

Variable	Notation	Units
Precipitation recycling ratio	ρ_r	
Precipitable water	PW	$\mathrm{mm\,d^{-1}}$
Low cloud	LC	
Precipitation	P	$\mathrm{mm\,d^{-1}}$
Zonal moisture flux	QU	$\mathrm{kg\,m^{-1}\,s^{-1}}$
Meridional moisture flux	QV	$\mathrm{kg\,m^{-1}\,s^{-1}}$
Moisture flux divergence	DV	$\mathrm{mm\,d^{-1}}$
Soil moisture	SM	$\mathrm{kg\,m^{-2}}$
Evaporation	E	$\mathrm{mm\,d^{-1}}$
Sensible heat flux	SH	$\mathrm{W\,m^{-2}}$
Surface air temperature	TM	K

not exceed one-third of the total length of the time series (Vautard *et al.*, 1992), a 10-year time-lag window was used to identify the dominant modes. A signal was regarded as robust only when it remained approximately invariant under the 8-year and 9-year window. To gain a detailed insight into the changes of land–atmosphere variables and precipitation recycling variability, M-SSA was also used to extract the spatial pattern of each variable through reconstructing specific modes in grid space. The temporal evolution of the mode could also be observed through reconstructing the signal at consecutive time levels.

3. Results and discussion

3.1. The climate background of arid and semi-arid China

Considering the definitions of climate zones presented by Wang and Ho (2002) and Zheng *et al.* (2010), the arid and semi-arid regions were defined as areas with annual precipitation below 500 mm. As shown in Figure 1, the studied region mainly included the provinces of Xinjiang, Inner Mongolia, Gansu and Ningxia, as well as the north of Qinghai Province, which is mostly located at 1000–4000 m above sea level. This region is mainly dominated by westerly flow and is not greatly influenced by the Asian monsoon (Wang and Ho, 2002; Ding and Chan, 2005).

The regional average time series of precipitation (P), evaporation (E), the net inflow of water moisture into the analysed region (W_{IN}), the recycling ratio (ρ_r) and the precipitation efficiency (χ) during the warm season from 1979 to 2010 are shown in Figure 2(a)–(e). As we can see, increasing trends are almost consistent for the four variables, except for W_{IN} before the beginning of the 1990s. With a simple analysis of the linear trends for these variables during the three decades, i.e. 1979–1989, 1990–1999 and 2000–2010, it can be seen that obvious increasing trends occur in the first decade and the last decade for the four variables. But in the second decade, weak downward trends dominate most variables, except precipitation, which shows a slight increasing trend. The trends of ρ_r match well with those of W_{IN} and E, i.e. an increasing recycling ratio corresponds to increasing evaporation but decreasing advected water, and vice versa.

Dirmeyer and Brubaker (2007) found that precipitation recycling appears to be relatively high over interior China at the annual and seasonal scale and that areas of high terrain tend to stand out as having high recycling ratios (Dominguez *et al.*, 2006; van der Ent *et al.*, 2010). The combination of low precipitable water over the high terrain and high warm-season reanalysis evaporation rates may cause the high recycling ratio (Dominguez *et al.*, 2006; Dirmeyer and Brubaker, 2007). This is also the case for our study region, as shown by Figures 1 and 2(d). Although the estimates of the recycling ratio in some mountainous areas may be spurious, the high recycling ratio reaching 15–20% (Figure 2(d)) still indicates some basic characteristics of the hydrological cycle because the ocean moisture can barely stay in the air after travelling westward more than 3000 km on average to the inland area studied here.

Highly consistent variations appear in ρ_r and χ, with a correlation coefficient between them of about 0.73

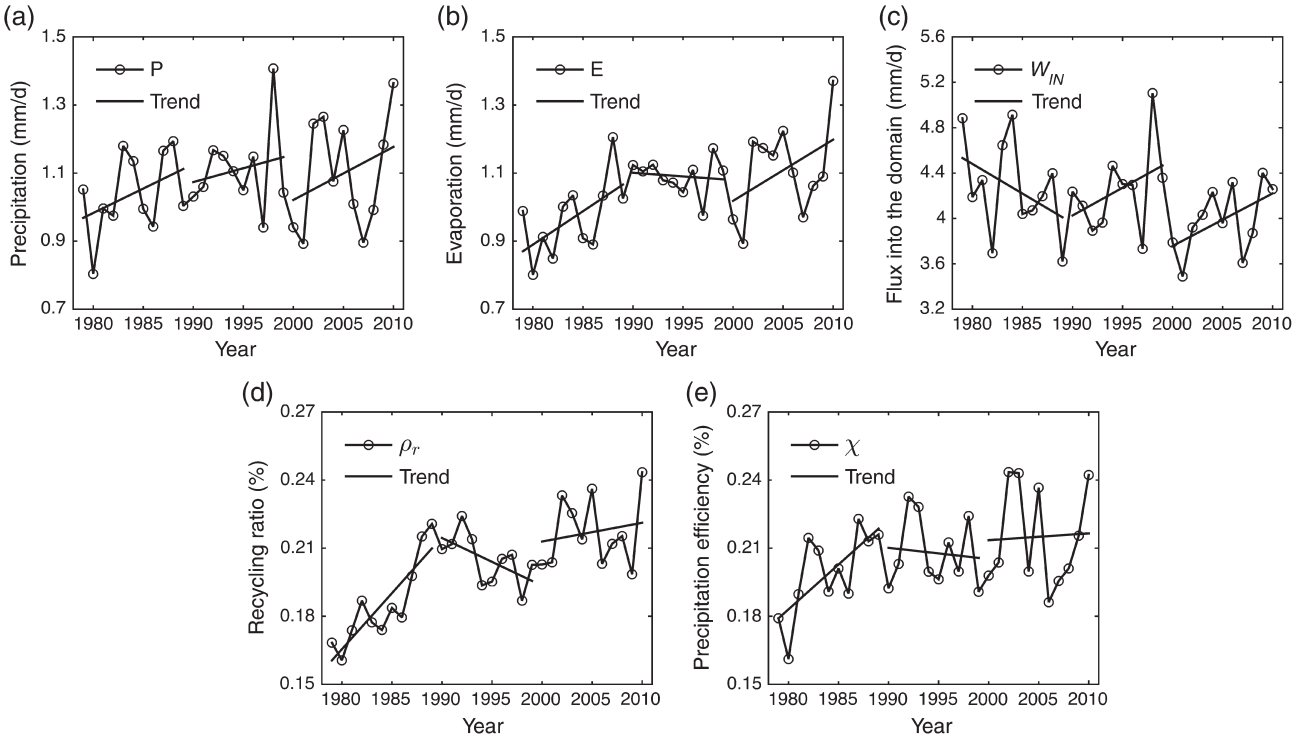

Figure 2. Regional average time series of (a) precipitation, (b) evaporation, (c) the moisture flux into the analysed domain, (d) the recycling ratio and (e) precipitation efficiency. Each panel also shows their linear trends for the three decades of 1979–1989, 1990–1999 and 2000–2010 (solid lines).

(Figure 2(d) and (e)). From the work on Europe by Schär *et al.* (1999), regional climate modelling revealed that the indirect processes are more important than the direct processes for precipitation variation (Asharaf *et al.* 2012). In their experiment, the moisture fluxes entering the analysed domain of France were about 14 times larger than the regional evaporation. According to Equation (4), only small changes in precipitation efficiency could explain most of the changes in precipitation due to the large amount of available water. Unlike the European region, our study region has a W_{IN} value of only four times that of E, approximately (Figure 2(b) and (c)). Therefore, the long-term trend of precipitable water depends on the trends of both W_{IN} and E. Because of limited amounts of available water for precipitation and a relatively higher proportion of regional evaporation, the precipitation variation in the arid/semi-arid regions depends more on the direct processes than it does in wet regions, especially with the stronger relation to evaporation, as well as the recycling processes. This is why the precipitation efficiency correlates highly with the recycling ratio. In short, the recycling process is very important for both the direct and indirect processes in the arid and semi-arid regions studied here.

3.2. M-SSA results: temporal variability

From the results of the M-SSA for the joint field consisting of the 32-year time series of 11 variables are listed in Table 1, significant oscillatory components were not captured, while the nonlinear trend components were detected. It should be pointed out that the advantage of using M-SSA is that nonlinear trends are generated from the lagged covariance matrix of all variables (Krishnamurthy and Krishnamurthy, 2014). The dominant nonlinear trend explains about 37.2% of variance for the joint field. Figures 3–5 present the time series reconstructed from the nonlinear trend modes and their relationships with ρ_r. Here, the variables joining M-SSA are classified into three groups: the first group (Figure 3) mainly includes atmospheric variables, such as precipitable water (*PW*), low-cloud cover (*LC*) and precipitation (*P*); the second group (Figure 4) represents flux and divergence variables including zonal and meridional moisture flux (*QU* and *QV*) and moisture flux divergence (*DV*); and the final group (Figure 5) consists of land variables – namely, soil moisture content (*SM*), evaporation (*E*), sensible heat (*SH*) and surface air temperature (*TM*).

(1) Covariation characteristics of the recycling ratio and atmospheric variables

An impressive result presented by Figures 3–5 is the apparent bimodal trend for ρ_r (dotted lines), with peaks at around 1991 and 2004. Figure 3 shows relationships between ρ_r and atmospheric variables. As we can see from Figure 3(a), there is remarkably similar variation between ρ_r and *PW*, with their correlation coefficient of 0.45 passing the 99% significance test. As mentioned above, the contribution percentage of local moisture is greater in the lower troposphere and less in the middle and upper troposphere (Bosilovich 2003; Burde, 2006). Although this phenomenon addresses the drawback of the well-mixed assumption adopted by the DRM, it also points out the close relationship between evaporated moisture and low cloud. As Cook *et al.* (2006) emphasized, increased soil moisture can result in an increased latent heat flux and increased moisture in the lower atmosphere and low cloud. This is confirmed by the fact that ρ_r follows almost the

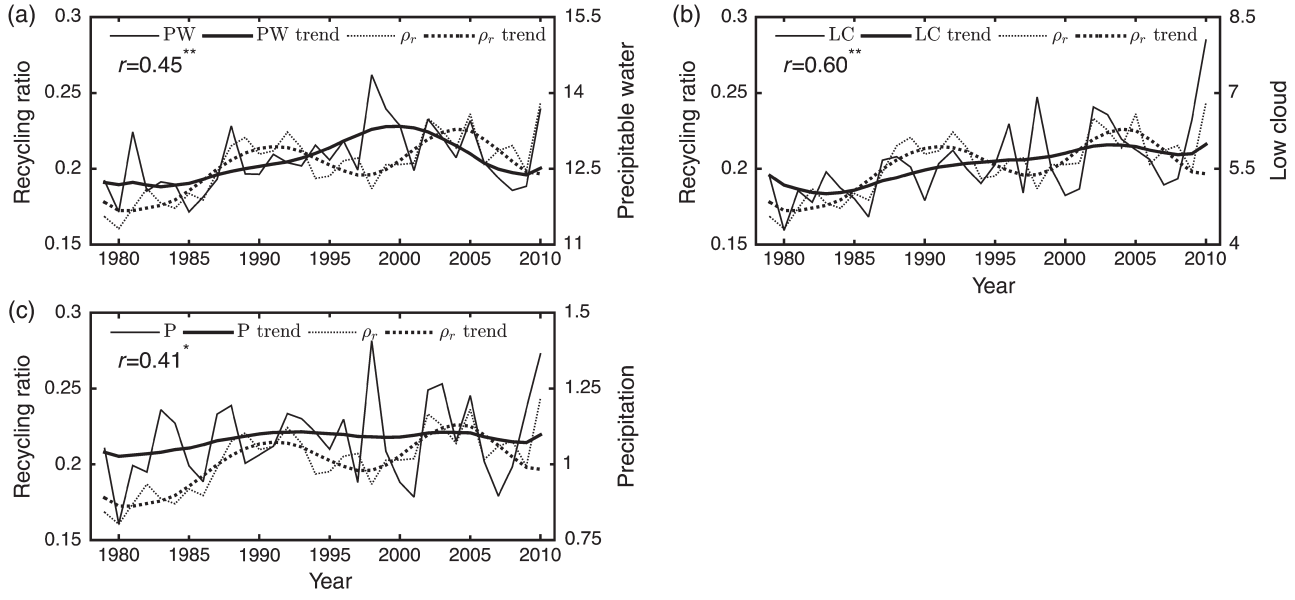

Figure 3. Time series of the recycling ratio (light dotted lines) and variables (light solid lines) related with atmospheric variables and their reconstructed nonlinear trend time series (bold dotted and solid lines) from 1979 to 2010. The correlation coefficients between the original time series of the recycling ratio and the other variables are also presented in each panel. The explained variance of nonlinear trend modes is about 37.2% for the joint field composed of all 11 fields in Table 1. The superscripts '**' and '*' denote statistical significance at the 99% and 90% confidence level, respectively. Units: same as those in Table 1.

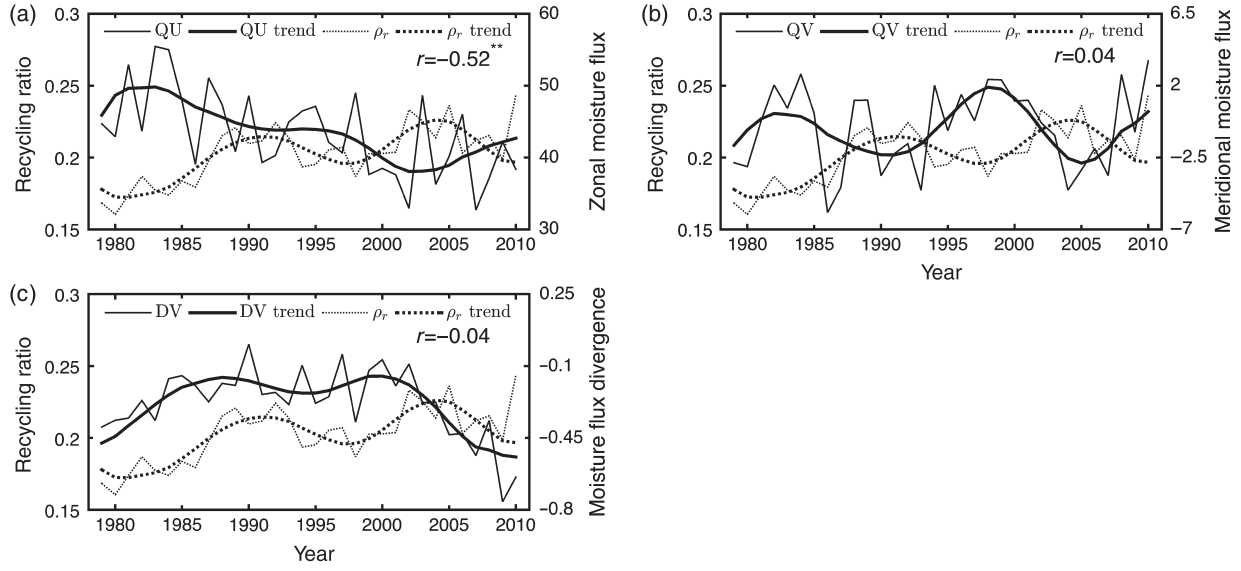

Figure 4. As in Figure 3 but for flux and divergence variables.

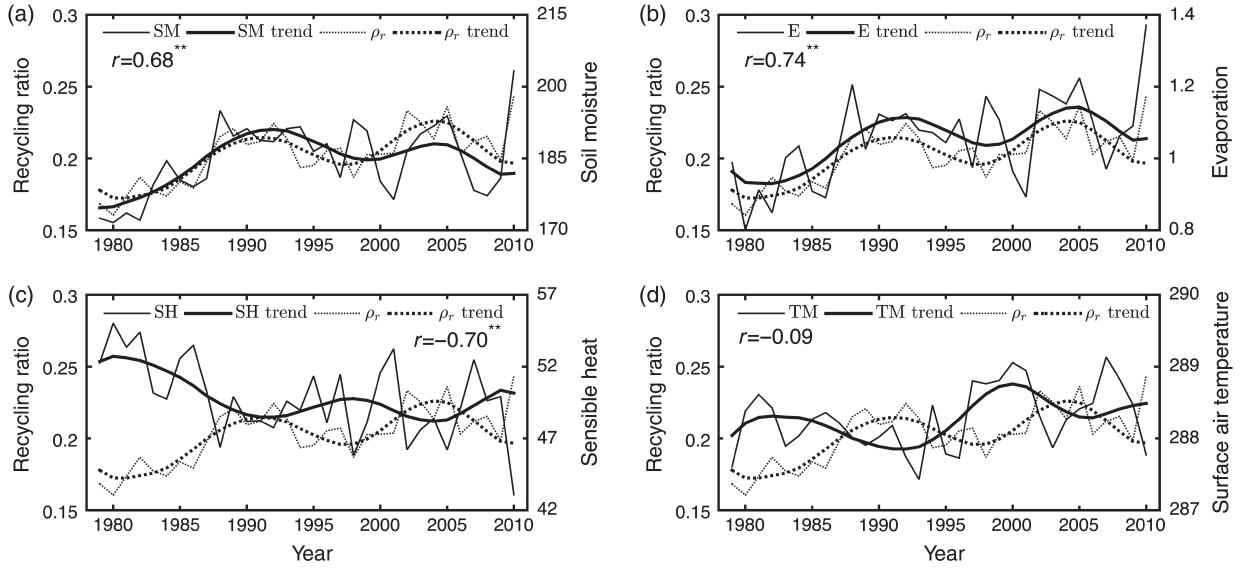

Figure 5. As in Figure 3 but for land and energy variables.

same trend as evaporation (Figure 5(b)) and low cloud (Figure 3(b)). The correlation coefficient between ρ_r and *LC* reaches 0.6 at the greater than 99% confidence level. At the same time, there are relatively weaker correlations between ρ_r and the mid- and high-level cloud cover (figures omitted).

Figure 3(c) shows the in-phase trends of precipitation and the recycling ratio. A different relationship was reached over the central U.S. plains (Dominguez and Kumar, 2008), where a significant negative correlation was found between precipitation recycling and precipitation. That study indicated that the precipitation was primarily composed of the advected moisture from large-scale convergence, but the evaporation moisture contribution became dominant only when the advected moisture diminished. However, over the arid and semi-arid regions of China, as precipitation increases, soil moisture and evaporation increase accordingly (Figure 5(a) and (b)) to provide more water to the overlying atmosphere. Meanwhile, the amount of precipitable water increases and supports the formation of low-level cloud and convective precipitation, promoting the development of recycled precipitation. To summarize, over the arid and semi-arid regions of China, the recycling ratio is generally enhanced during periods of increased precipitable water, low-cloud cover and precipitation.

(2) Covariation characteristics of the recycling ratio and flux and divergence variables

Information on external moisture transport can be displayed by the dynamical transport variables, such as zonal moisture flux, meridional moisture flux and moisture divergence (Figure 4(a)–(c)). The characteristics

of atmospheric circulation can be seen in QU and QV (Figure 4(a) and (b)). It appears that the direction of horizontal moisture transport is a major factor for recycling, compared with any other, because there is eastward moisture transport by prevailing westerlies in the midlatitudes. The east–west long but north–south narrow region selected in this work also possibly enhances the effect of westerly moisture flux. And the westerly moisture flux (positive QU) shows a clear decreasing trend from the middle period of the 1980s to the beginning of the 2000s (Figure 4(a)). But for QV, although its magnitude is of almost two orders smaller than QU, the trend of QV fluctuates around zero mean with amplitude comparable to that of QU. For the long-term trend, the northerly (negative)/southerly (positive) moisture flux corresponds to high/low ρ_r (Figure 4(b)). The significant negative $\rho_r \sim QU$ correlation also indicates that large values of moisture transport suppress precipitation recycling. So, it can be concluded that the long-term increasing trend of ρ_r may be caused by the gradually decreasing westerly. But, the bimodal structure upon the long-term trend of ρ_r may be modulated by the fluctuations of the meridional moisture flux, whose positive phase (southerly) tends to reduce the contribution from the recycling process through bringing more moisture into the study region from the ocean and wetlands in the south.

The moisture flux divergence (DV) tendency (Figure 4(c)) displays the presence of a persistent moisture sink, i.e. negative DV. The DV and ρ_r have a weak negative correlation coefficient of -0.04 (not statistically significant). Furthermore, the regional mean absolute value of the divergence term ($-0.28\,\mathrm{mm\,d^{-1}}$) is smaller than the evaporation ($1.05\,\mathrm{mm\,d^{-1}}$) across the whole region, suggesting that a considerable part of the moisture source for precipitation must come from regional evaporation. On the other hand, the studied region generally being a moisture sink is also reflected by the summer regional average precipitation rate ($1.08\,\mathrm{mm\,d^{-1}}$) being larger than evaporation, i.e. $P > E$. Combined with the one-order weaker moisture convergence ($-0.28\,\mathrm{mm\,d^{-1}}$), this further confirms the important role of the recycling process for the hydrological cycle in the study region.

(3) Covariation characteristics of the recycling ratio and land and energy variables

There is a saying that 'rain follows the plow', reflecting the fact that a change in regional soil moisture affects the atmosphere. Many studies (Schär *et al.*, 1999; Hohenegger *et al.*, 2009; Seneviratne *et al.*, 2010; Asharaf *et al.*, 2012) have investigated the mechanisms controlling this soil moisture–precipitation feedback process. Soil moisture plays a key role in both the water and energy cycles, and its effect on land energy and water balances manifests in its impact on evaporation (Seneviratne *et al.*, 2010). Furthermore, Serafini (1990) pointed out that the soil moisture–evaporation feedback mechanism is likely to be particularly efficient in the interior of continents, just as in the area in the present study.

As shown by Figure 5(a), there is a close positive correlation between soil moisture and the recycling ratio in the arid and semi-arid regions of China. Just as Seneviratne *et al.* (2010) concluded, two regimes drive the process of evaporation, i.e. the soil moisture-limited regime and the energy-limited regime. For the arid and semi-arid regions, the generally moisture-limited condition cannot provide enough water for evaporation, whose change could thus significantly influence precipitation recycling and subsequently affect precipitation.

In wet regions, precipitation recycling becomes important only during periods experiencing low total precipitation (Berbery *et al.*, 2003; Bosilovich and Chern, 2006; Dominguez and Kumar, 2008). However, evaporation is low in the arid and semi-arid regions of China (Figure 5(b)). Although quantifying the relationship between soil moisture and atmospheric is difficult, soil moisture may have a controlling effect on evaporation (Dirmeyer *et al.*, 2012). As shown by Figure 5(b), a strong positive correlation of 0.74 exists between E and ρ_r, which suggests that surface moisture contributes directly to precipitation by providing evaporation. Recalling the weak net moisture transport mentioned above (Figure 4(c)), it necessarily results in a high regional recycling ratio. Together with the consistent variation and trend between soil moisture and evaporation shown in Figure 5(a) and (b), a strong positive relationship between land and atmosphere in the study region could be reached.

In addition, the increase in evaporation inevitably causes a decreasing of SH. Consequently, a strong negative relationship emerges between SH and ρ_r (Figure 5(c)). Temperature is another important energy variable affecting potential evaporation due to high temperature generally strengthening the process of water moisture leaving the land. However, water is a more important factor than energy in soil moisture-limited regions, like the region studied here. Therefore, a weak negative correlation between TM and ρ_r is apparent (Figure 5(d)).

3.3. M-SSA results: spatial variability

Figure 6 presents the spatial pattern of the trend mode of each variable in Table 1. To indicate the distribution of the recycling ratio in the studied region, the local recycling ratio (ρ_i) in Equation (2), rather than the recycling ratio (ρ_r), is shown. And the field of each reconstructed trend in Figure 6 has been normalized by itself so that all patterns in Figure 6 have values varying between -1 and 1.

Interestingly, similar increasing trends of ρ_i, PW, LC, P, QV, SM and E emerge in the western and central parts of the study region, but opposite tends are apparent in the remaining part. To some degree, the result is similar to previous studies (e.g. Shi *et al.*, 2003; Ma and Fu, 2005), in which an increasing wetting tendency is apparent in the west of northwest China. The meridional boundary dividing these two parts is at approximately 110°E, except that the positive trend of ρ_i extends more to the east. Meanwhile, the reverse spatial distribution of the trend is found in the DV, SH and TM fields, i.e. a decrease in the west

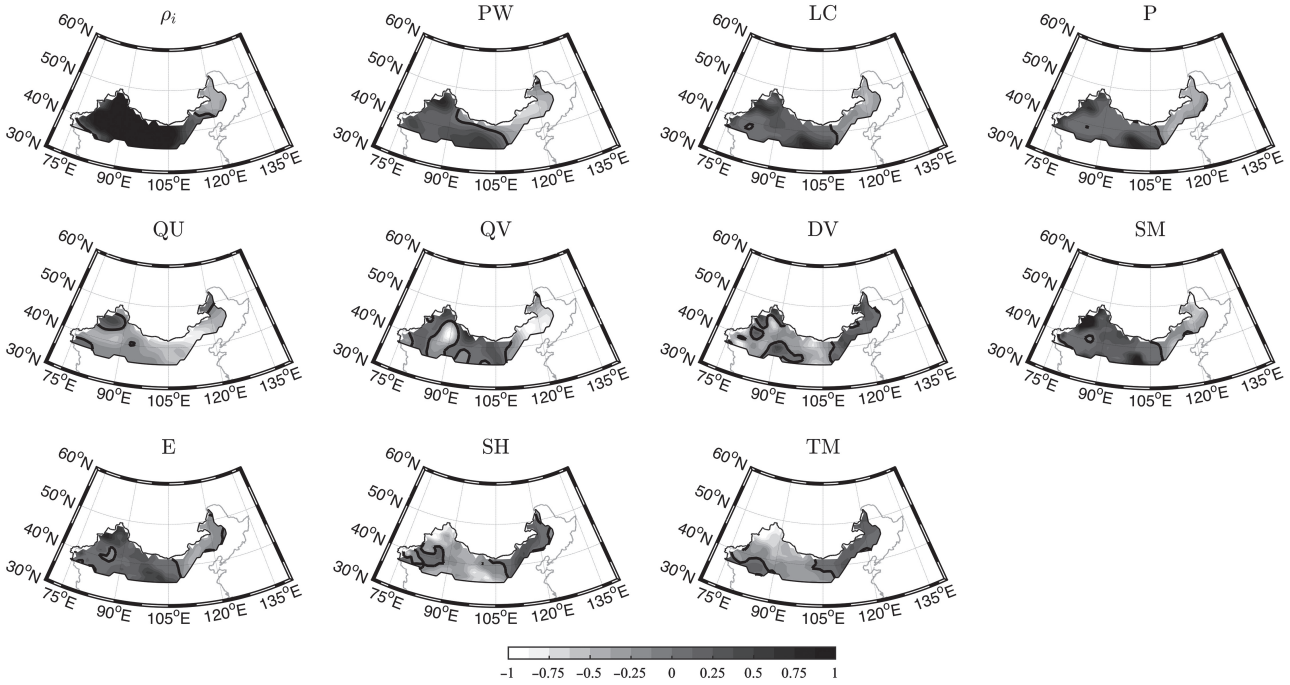

Figure 6. Spatial patterns of trend modes for land–atmosphere variables. Each pattern has been normalized by itself to vary between −1 and 1.

and an increase in the east. Another feature is a decrease in *QU*, over almost the entire region, during the analysis period, which confirms the consistent weakening trend of westerly moisture transport throughout the study region in Figure 4(a). Even though westerly vapour flux decreases during 1979–2010, an increasingly strengthened moisture sink effect (negative divergence of moisture flux) exists in most areas of the western part. This corresponds to the increases in soil moisture and evaporation west of 110°E. Additionally, the increasing trend in precipitation recycling and precipitation there suggests that the positive relationship between soil and precipitation will provide moisture for recycled precipitation and further support the water supply for regional precipitation.

To further understand the difference in the long-term variability between the west and east part of the analysed region, the simple linear trends of the variables listed in Table 1 were separately calculated for the two sub-regions and the whole region (Table 2). It should be noted that the recycling ratio in the western part is obviously larger than the eastern part due to the relatively larger area of the western part (Dominguez *et al.*, 2006; van der Ent *et al.*, 2010); the regional means of the local recycling ratio (ρ_i) are therefore listed in Table 2.

In Table 2, the time-mean values of most variables are lower in the western part (arid region) than in the eastern part (semi-arid region), except for mean ρ_i. This reflects the basic climate difference between arid and semi-arid regions. Another clear characteristic is the opposite trends of these variables in the two parts of the region. As with the characteristics revealed by the nonlinear trend of ρ_i in Figure 6, the spatially averaged ρ_i also displays a distinct ascending trend in the west and a weak declining trend in the east. For the western part, a homogeneous ascending trend is found for *PW*, *LC*, *P*, *QV*, *SM*, *E* and *TM* (not statistically significant), while an out-of-phase trend is present for the variables *QU*, *DV* and *SH*. For all variables except *QU* and *TM*, the linear trend is opposite in sign in the west and east. *TM* displays an increasing trend in both parts of the study region, especially in the east. At the same time, the westerly moisture transport tends to weaken in both parts. Together with the moisture flux convergence (negative *DV*) strengthening in the west but weakening in the east, we can conclude that the eastern part (semi-arid area) of the study region has a more obvious drying and warming tendency.

Although *P* shows no significant increasing trend throughout the entire region (Table 2), a significant increasing/decreasing trend at the greater than 99% confidence level is apparent in the west/east sub-region. Figure 7 further presents the relationship between precipitation and moisture flux in the two sub-regions. For both sub-regions, westerly moisture transport decreases (Figure 7(a) and (b)), while southerly/northerly moisture transport strengthens in the west/east sub-region (Figure 7(c) and (d)). And in the eastern part, the southerly moisture flux reaches a very high level in the early 1980s, when the positive *QV* is about three times larger than usual. Also in the early 1980s, the amount of southerly moisture flux is comparable to the westerly moisture flux in the eastern part. Except for that period, the westerly moisture flux dominates the water transport throughout the whole region.

As shown in Figure 7(e) and (f) and Table 2, the moisture flux divergence shows a significant decreasing and weak increasing trend in the west and east sub-region, respectively. For the western part, the increasing moisture sink, soil moisture and evaporation (Figure 6 and Table 2) imply

Table 2. Time means (represented by 'Mean' in the table) and linear trends (represented by 'Trend' in the table; units: /10 year) of the variables listed in Table 1, during 1979–2010, for the whole study region and the two sub-regions.

	Whole region			West sub-region			East sub-region		
Variable	Mean	Trend	FP	Mean	Trend	FP	Mean	Trend	FP
ρ_i	0.22	**0.01**	0	0.25	**0.03**	0	0.13	−0.004	0.12
PW	12.70	**0.27**	0.02	11.52	**0.42**	0	16.17	−0.18	0.24
LC	0.06	**0.005**	0	0.05	**0.009**	0	0.07	**−0.008**	0
P	1.08	0.04	0.14	0.85	**0.12**	0	1.78	**−0.22**	0
QU	43.36	**−3.49**	0	35.41	**−3.34**	0	66.89	**−3.93**	0.03
QV	−0.65	0.31	0.52	−2.13	**2.38**	0	3.70	**−5.81**	0.01
DV	−0.28	**−0.06**	0.05	−0.29	**−0.11**	0	−0.24	0.08	0.28
SM	184.82	**3.44**	0.01	126.62	**8.02**	0	357.17	**−10.12**	0
E	1.05	**0.07**	0	0.86	**0.14**	0	1.63	**−0.13**	0
SH	49.76	**−1.45**	0	49.68	**−3.06**	0	50.02	**3.33**	0
TM	288.28	**0.15**	0.06	288.23	0.02	0.80	288.42	**0.55**	0

The abbreviation 'FP' is the corresponding p value of the trend's F-test. Trends significantly different from zero at the 90% confidence level are set in bold. The units for each variable can be found in Table 1.

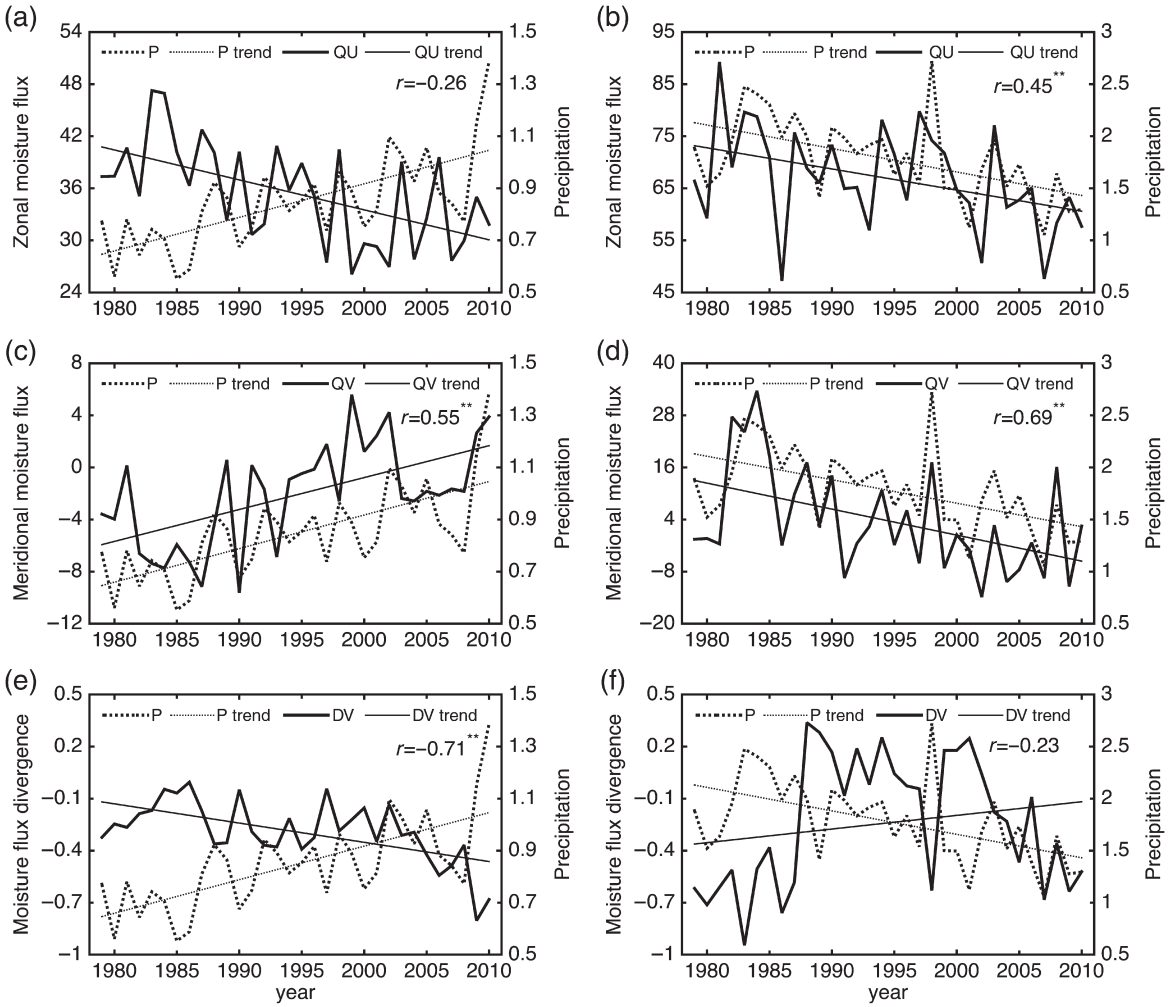

Figure 7. Regional averaged time series of precipitation- and moisture transport–related variables for (a, b) zonal moisture flux, (c, d) meridional moisture flux and (e, f) moisture flux divergence in the (a, c, e) western and (b, d, f) eastern sub-region. The two sub-regions are divided with respect to the meridional boundary at 110°E. The linear trend of each variable is represented by the straight line with the same line type as its original series. The correlation coefficient between the precipitation and moisture transport variable is presented in each panel. The superscript '**' indicates statistical significance at the 99% confidence level. Units: same as those in Table 1.

that increasing converged moisture promotes soil water and regional evaporation, which contributes to regional precipitation through the recycling process. On the other hand, precipitation in turn controls the water content in the soil in the dry area. Therefore, the change in evaporation is strongly sensitive to precipitation variation (Wang and Zeng, 2011).

Wei and Wang (2013) studied the average temperatures of 47 observation stations in northwest China. Their research showed a continuous warming in the region since the early 1970s. A slight/significant increasing linear trend of air temperature is also apparent over the west/east sub-region in the present study (Table 2). Because evaporation is affected greatly by temperature, increasing temperature will enhance evaporation when there is sufficient moisture available in the soil. Otherwise, dry soil cannot continue to supply moisture to the overlying atmosphere.

3.4. Discussion

Based on the above analysis, the characteristics of the water cycle in the arid/semi-arid regions of China are summarized schematically in Figure 8. From the point of view of atmospheric moisture transport, there is a consistent trend of decreasing/increasing westerly/easterly moisture transport in both the western and eastern parts of the study region. However, the opposite trend for meridional transport, i.e. increasing/decreasing southerly/northerly moisture transport in the western sub-region and the reverse in the eastern sub-region, is one order of magnitude smaller than for zonal transport (Figure 7(a)–(d)). Under this kind of moisture transport, the moisture flux convergence has an increasing/decreasing trend in the western/eastern part (Figure 7(e) and (f)). The transport of water in the air further results in an increasing/decreasing trend of precipitable water, low cloud and then precipitation in the western/eastern part. Through the precipitation–soil moisture interaction process, the trend in soil moisture is also the reverse in the two parts of the study region. This enhances/weakens evaporation and inhibits/promotes sensible heat in the western/eastern sub-region. The precipitation recycling in the western/eastern sub-region is therefore reinforced/weakened during the 32-year period, which suggests the precipitation in the western/eastern sub-region tends to gain a higher/lower proportion of moisture from regional evaporation through the evaporation–precipitation interaction process. Additionally, the increasing/decreasing trends of the recycling ratio, evaporation and soil moisture imply that precipitation in the arid/semi-arid areas is highly sensitive to soil moisture content, i.e. there is a strong 'S–P' (soil moisture–precipitation) interaction process in the arid and semi-arid regions of China.

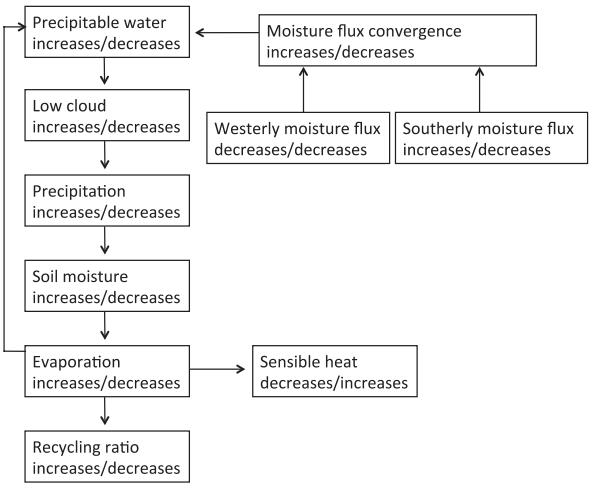

Figure 8. Schematic diagram of land–atmosphere interaction processes in the arid and semi-arid regions of China during 1979–2010. The 'decreases' or 'increases' on the left (right) of the '/' symbol represent the long-term trends of related variables in the western (eastern) sub-region. See Section 3.4 in the main text for details.

Also, as shown in Figure 8, a direct and distinct positive relationship between precipitation and soil moisture is generally apparent. In terms of soil moisture–evaporation interaction, Seneviratne *et al.* (2010) pointed out that a positive relationship occurs in transitional regions between dry and wet climates (Koster *et al.*, 2004). However, if the enhancement in precipitation cannot meet the increase in evaporation, the potential for negative feedback exists. Although the region analysed is not completely coincident with the land–atmosphere interaction 'hot spots' addressed by Koster *et al.* (2004) and Zhang *et al.* (2008), an obvious and positive soil moisture–evaporation relationship still exists.

Just as Seneviratne *et al.* (2010) stressed in their research, the evaporation–precipitation process in Figure 8 is the most uncertain link. In the region studied here, there is positive coupling between soil moisture and precipitation during the warm season over a long time scale. That means strong precipitation recycling in the study region, especially in the western sub-region.

Wei and Wang (2013) found an anomalous easterly in northwestern China during recent decades. They suggested the strengthened easterly could reduce the water vapour transport from the midlatitude westerly. Together with the strengthened evaporation resulting from the continuous rise in temperature, intensified drought condition have occurred in northwestern China. However, as the above analysis for the western part of the study region shows, although westerly moisture transport displays a decreasing trend, southerly moisture transport and moisture flux convergence are increasing. The increasing soil moisture and rising air temperature result in stronger evaporation and larger amounts of moisture move into the atmosphere, which contributes to the increases in regional recycled precipitation. This is consistent with the increasing trend in the recycling ratio in the western sub-region. Gao *et al.* (2007) also pointed out that the increasing annual precipitation trend drives the increasing trend of actual evapotranspiration, accompanied by increasing air temperature in western China. On the contrary, for the eastern sub-region, under the conditions of reducing advected moisture and decreasing evaporation moisture, and simultaneously with rising temperature, the climate will change to one that is warm and dry.

4. Conclusion

Precipitation recycling is an important process in understanding the hydrological cycle. The dynamic recycling model (DRM), including moisture storage, is a good quantitative tool to estimate land–atmosphere interaction (Bisselink and Dolman, 2008). The work reported in this paper applied the DRM presented by Dominguez *et al.* (2006) to derive the regional precipitation recycling ratio across the arid and semi-arid regions of China, using JRA-25 reanalysis data. In addition, the multivariate spectral method was used to extract nonlinear trends common to 11 land–atmosphere interaction variables, to display characteristics of the land surface and its interaction with the atmosphere in the warm season from 1979 to 2010.

For the physical variables regionally related to precipitation, such as evaporation, the recycling ratio and precipitation efficiency, increasing trends are apparent, especially in the period before the 1990s. However, for the variables closely related to external moisture transport, such as the net water flux into the region, decreasing trends during 1979–2010 are clear. Significant correlation between precipitation efficiency and the recycling ratio reveals precipitation recycling is efficient and should not be ignored for the precipitation over the analysed region, due to its relatively low level of advected moisture.

Positive soil moisture–precipitation interaction was found in the arid and semi-arid regions of China. That is, an enhanced recycling ratio occurred with increased precipitable water, low-cloud cover, precipitation, soil moisture and evaporation, while westerly moisture transport weakened, during the study period. Furthermore, evaporation was strongly influenced by regional soil moisture and its trend clearly affected precipitation recycling.

Besides the covariation characteristics of the entire analysed region, an interesting finding of this study is the reverse tendencies of land and atmospheric variables in the western and eastern parts of the arid and semi-arid regions of China. For the sub-region west of 110°E, the analysis showed that increased southerly moisture flow strengthens the precipitable water in the atmosphere and favours the formation of precipitation. At present, decreasing westerly moisture flow has little influence upon regional precipitation. As a result, the abundant precipitable water is conducive to cloud formation and precipitation, wetting of soil moisture, feeding more moisture into the atmosphere, and increasing the recycling ratio. Furthermore, temperature is slightly increasing, shown by the linear trends, and the wetting of soil moisture supports a higher precipitation recycling and displays positive land–atmosphere interaction. This implies that the present climate is becoming wetter in the western sub-region of the arid and semi-arid regions of China. However, the opposite tendency was found in the rest of the study region: weakening advected moisture convergence with both westerly and southerly moisture transport decreasing, and less evaporation and warming temperatures causing the climate to shift towards warm and dry conditions.

This study proposes a view of regional land–atmosphere interaction and the possible climatic change mechanism in the arid and semi-arid regions of China. Although the impacts of other related variables, such vegetation or land cover, were not included in the discussion of this study, it does not mean that they are unimportant in modulating the surface water and energy balance. Additionally, the decision to use a reanalysis dataset to study the potential interaction between land and atmosphere was largely due its comprehensiveness compared with observational data. However, reanalysis also suffers from problems, such as the lack of water mass conservation due to data assimilation. Therefore, observation-based investigations would be the most direct way to study and verify the results of the present study. Furthermore, considering the complexity of land–atmosphere feedback, the causal relationships between different processes involved in such feedback are hard to elucidate. This study only presents a possible relationship between land and atmosphere over a long time scale in the arid and semi-arid regions of China; the same relationship will not necessarily hold true at temporal and spatial scales different from those analysed here.

Acknowledgements

This work was supported by the National Natural Science Foundation of China (NSFC) under grant nos. 41475072, 41275064 and 40905037, the China Meteorological Administration R&D Special Fund for Public Welfare (Meteorology) under grant no. GYHY201306024, and the National Department Public Benefit Research Foundation of Ocean under grant no. 201005019. We also appreciate the useful comments from the anonymous reviewers, which contributed to improving the manuscript.

References

Alfieri L, Claps P, D'Odorico P, Laio F, Over TM. 2008. An analysis of the soil moisture feedback on convective and stratiform precipitation. *J. Hydrometeorol.* **9**: 280–291, doi: 10.1175/2007JHM863.1.

Asharaf S, Dobler A, Ahrens B. 2012. Soil moisture–precipitation feedback process in the Indian summer monsoon season. *J. Hydrometeorol.* **13**: 1461–1474, doi: 10.1175/JHM-D-12-06.1.

Bagley JE, Desai AR, Harding KJ, Snyder PK, Foley JA. 2014. Drought and deforestation: has land cover change influenced recent precipitation extremes in the Amazon? *J. Clim.* **27**: 345–361, doi: 10.1175/JCLI-D-12-00369.1.

Berbery EH, Luo Y, Mitchell KE, Betts AK. 2003. Eta model estimated land surface processes and the hydrologic cycle of the Mississippi basin. *J. Geophys. Res.* **108**: 8852, doi: 10.1029/2002JD003192.

Betts AK, Ball JH, Beljaars ACM, Miller MJ, Viterbo PA. 1996. The land surface–atmosphere interaction: a review based on observational and global modeling perspectives. *J. Geophys. Res.* **101**: 7209–7225.

Bisselink B, Dolman AJ. 2008. Precipitation recycling: moisture sources over Europe using ERA-40 data. *J. Hydrometeorol.* **9**: 1073–1083.

Bisselink B, Dolman AJ. 2009. Recycling of moisture in Europe: contribution of evaporation to variability in very wet and dry years. *Hydrol. Earth Syst. Sci. Discuss.* **6**: 3301–3333.

Blanke B, Raynaud S. 1997. Kinematics of the Pacific Equatorial Undercurrent: an Eulerian and Lagrangian approach from GCM results. *J. Phys. Oceanogr.* **27**: 1038–1053.

Bosilovich MG. 2003. On the vertical distribution of local and remote sources of water for precipitation. *Meteorol. Atmos. Phys.* **80**: 31–41.

Bosilovich MG, Chern J. 2006. Simulation of water sources and precipitation recycling for the Mackenzie, Mississippi, and Amazon River basins. *J. Hydrometeorol.* **7**: 312–329.

Bosilovich MG, Schubert SD. 2001. Precipitation recycling over the central United States diagnosed from the GEOS-1 Data Assimilation System. *J. Hydrometeorol.* **2**: 26–35.

Bosilovich MG, Robertson FR, Chen J. 2011. Global energy and water budgets in MERRA. *J. Clim.* **24**: 5721–5739, doi: 10.1175/2011JCLI4175.1.

Broomhead DS, King GP. 1986. On the qualitative analysis of experimental dynamical systems. *Nonlinear Phenomena Chaos* **11**: 2530–2555.

Brubaker KL, Entekahabi D, Eagleson PS. 1993. Estimation of precipitation recycling. *J. Clim.* **6**: 1077–1089.

Brubaker KL, Dirmeyer PA, Sudradjat A, Levy BS, Bernal F. 2001. A 36-yr climatological description of the evaporation sources of warm-season precipitation in the Mississippi River Basin. *J. Hydrometeorol.* **2**: 537–557.

Brutsaert W, Parlange MB. 1998. Hydrologic cycle explains the evaporation paradox. *Nature* **396**: 30, doi: 10.1038/23845.

Budyko MI, Miller DH. 1974. *Climate and Life*. Academic Press: New York, NY and London.

Burde GI. 2006. Bulk recycling models with incomplete vertical mixing. Part I: conceptual framework and models. *J. Clim.* **19**: 1461–1472.

Chase TN, Pielke RA, Knaff JA, Kittel TGF, Eastman JL. 2000. A comparison of regional trends in 1979–1997 depth-averaged tropospheric temperatures. *Int. J. Climatol.* **20**: 503–518.

Chen YY, Yang K, He J, Qin J, Shi JC, Du JY, He Q. 2011. Improving land surface temperature modeling for dry land of China. *J. Geophys. Res.* **116**: D20104, doi: 10.1029/2011JD015921.

Cook BI, Bonan GB, Levis S. 2006. Soil moisture feedbacks to precipitation in southern Africa. *J. Clim.* **19**: 4198–4206.

Ding YH, Chan JCL. 2005. The East Asian summer monsoon: an overview. *Meteorol. Atmos. Phys.* **89**: 117–142, doi: 10.1007/s00703-005-0125-z.

Dirmeyer PA, Brubaker KL. 2007. Characterization of the global hydrologic cycle from a back-trajectory analysis of atmospheric water vapor. *J. Hydrometeorol.* **8**: 20–37, doi: 10.1175/JHM557.1.

Dirmeyer PA, Schlosser CA, Brubaker KL. 2009. Precipitation, recycling, and land memory: an integrated analysis. *J. Hydrometeorol.* **10**: 278–288, doi: 10.1175/2008JHM1016.1.

Dirmeyer PA, Cash BA, Kinter III JL, Stan C, Jung T, Marx L, Towers P, Wedi N, Adams JM, Altshuler EL, Huang B, Jin EK, Manganello J. 2012. Evidence for enhanced land–atmosphere feedback in a warming climate. *J. Hydrometeorol.* **13**: 981–995, doi: 10.1175/JHM-D-11-0104.1.

Dominguez F, Kumar P. 2008. Precipitation recycling variability and ecoclimatological stability – a study using NARR data. Part I: Central U.S. plains ecoregion. *J. Clim.* **21**: 5165–5186, doi: 10.1175/2008JCLI1756.1.

Dominguez F, Kumar P, Liang XZ, Ting MF. 2006. Impact of atmospheric moisture storage on precipitation recycling. *J. Clim.* **19**: 1513–1530.

Dominguez F, Kumar P, Vivoni ER. 2008. Precipitation recycling variability and ecoclimatological stability – a study using NARR data. Part II: North American monsoon region. *J. Clim.* **21**: 5187–5203, doi: 10.1175/2008JCLI1760.1.

Dorman JL, Sellers PJ. 1989. A global climatology of albedo, roughness length and stomatal resistance for atmospheric general circulation models as represented by the simple biosphere model (SiB). *J. Appl. Meteorol.* **28**: 833–855.

Draper C, Mills G. 2008. The atmospheric water balance over the semiarid Murray-Darling River basin. *J. Hydrometeorol.* **9**: 521–534, doi: 10.1175/2007JHM889.1.

Eltahir EAB, Bras RL. 1994. Precipitation recycling in the Amazon basin. *Q. J. R. Meteorol. Soc.* **120**: 861–880.

Eltahir EAB, Bras RL. 1996. Precipitation recycling. *Rev. Geophys.* **34**: 367–378.

Eltahir EAB, Pal JS. 1996. Relationship between surface conditions and subsequent rainfall in convective storms. *J. Geophys. Res.* **101D**: 26237–26245.

van der Ent RJ, Savenije HHG, Schaefli B, Steele-Dunne SC. 2010. Origin and fate of atmospheric moisture over continents. *Water Resour. Res.* **46**: W09525, doi: 10.1029/2010WR009127.

Findell KL, Eltahir EAB. 1997. An analysis of the soil moisture-rainfall feedback, base on direct observations from Illinois. *Water Resour. Res.* **33**: 725–735.

Fu CB, Wen G. 2002. Several issues on aridification in the northern China. *Clim. Environ. Res.* **7**: 22–29 (in Chinese).

Fu X, Xu XD, Kang HW. 2006. Research on precipitation recycling during Meiyu season over Middle-Lower Reaches of Changjiang River in 1998. *Meteorol. Sci. Technol.* **34**: 394–399 (in Chinese).

Gao G, Chen DL, Xu CY, Simelton E. 2007. Trend of estimated actual evapotranspiration over China during 1960–2002. *J. Geophys. Res.* **112**: D11120, doi: 10.1029/2006JD008010.

Ghil M, Allen M, Dettinger M, Ide K, Kondrashov D, Mann M, Robertson A, Saunders A, Tian Y, Varadi F. 2002. Advanced spectral methods for climatic time series. *Rev. Geophys.* **40**: 1003, doi: 10.1029/2000RG000092.

Gimeno L, Stohl A, Trigo RM, Dominguez F, Yoshimura K, Yu L, Drumond A, Durán-Quesada AM, Nieto R. 2012. Oceanic and terrestrial sources of continental precipitation. *Rev. Geophys.* **50**: RG4003, doi: 10.1029/2012RG000389.

Giorgi F, Mearns LO, Shields C, Mayer L. 1996. A regional model study of the importance of local versus remote controls of the 1988 drought and the 1993 flood over the central United States. *J. Clim.* **9**: 1150–1162.

Goessling HF, Reich CH. 2011. What do moisture recycling estimates tell us? Exploring the extreme case of non-evaporating continents. *Hydrol. Earth Syst. Sci.* **15**: 3217–3235, doi: 10.5194/hess-15-3217-2011.

Guillod BP, Orlowsky B, Miralles D, Teuling AJ, Blanken PD, Buchmann N, Ciais P, Ek M, Findell KL, Gentine P, Lintner BR, Scott RL, Van den Hurk B, Seneviratne SI. 2014. Land-surface controls on afternoon precipitation diagnosed from observational data: uncertainties and confounding factors. *Atmos. Chem. Phys.* **14**: 8343–8367, doi: 10.5194/acp-14-8343-2014.

Harding KJ, Snyder PK. 2012a. Modeling the atmospheric response to irrigation in the Great Plains. Part I: general impacts on precipitation and the energy budget. *J. Hydrometeorol.* **13**: 1667–1686, doi: 10.1175/JHM-D-11-098.1.

Harding KJ, Snyder PK. 2012b. Modeling the atmospheric response to irrigation in the Great Plains. Part II: the precipitation of irrigated water and changes in precipitation recycling. *J. Hydrometeorol.* **13**: 1687–1703, doi: 10.1175/JHM-D-11-099.1.

Hohenegger C, Brockhaus P, Bretherton CS, Schär C. 2009. The soil moisture–precipitation feedback in simulations with explicit and parameterized convection. *J. Clim.* **22**: 5003–5020, doi: 10.1175/2009JCLI2604.1.

Jones AR, Brunsell NA. 2009. Energy balance partitioning and net radiation controls on soil moisture–precipitation feedbacks. *Earth Interact.* **13**: 1–25, doi: 10.1175/2009EI270.1.

Kang HW, Gu XQ, Fu X, Xu XD. 2005. Precipitation recycling over the Northern China. *J. Appl. Meteorol. Sci.* **16**: 139–147 (in Chinese).

Koster RD, Jouzel J, Souzzo R, Russel G, Rind D, Eagleson PS. 1986. Global sources of local precipitation as determined by the NASS/GISS GCM. *Geophys. Res. Lett.* **13**: 121–124.

Koster RD, Dirmeyer PA, Guo Z, Bonan G, Chan E, Cox P, Gordon CT, Kanae S, Kowalczyk E, Lawrence D, Liu P, Lu C, Malyshev S, McAvaney B, Mitchell K, Mocko D, Oki T, Oleson K, Pitman A, Sud YC, Taylor CM, Verseghy D, Vasic R, Xue Y, Yamada T. 2004. Regions of strong coupling between soil moisture and precipitation. *Science* **305**: 1138–1140, doi: 10.1126/science.1100217.

Koster RD, Guo Z, Dirmeyer PA, Bonan G, Chan E, Cox P, Davies H, Gordon CT, Kanae S, Kowalczyk E, Lawrence D, Liu P, Lu C, Malyshev S, McAvaney B, Mitchell K, Mocko D, Oki T, Oleson KW, Pitman A, Sud YC, Taylor CM, Verseghy D, Vasic R, Xue Y, Yamada T. 2006. GLACE: The Global Land–Atmosphere Coupling Experiment. Part I: overview. *J. Hydrometeorol.* **7**: 590–610, doi: 10.1175/JHM510.1.

Krishnamurthy L, Krishnamurthy V. 2014. Decadal scale oscillations and trend in the Indian monsoon rainfall. *Clim. Dyn.* **43**: 319–331, doi: 10.1007/s00382-013-1870-1.

Liu D, Wang GL, Mei R, Yu ZB, Yu M. 2013. Impact of initial soil moisture anomalies on climate mean and extremes over Asia. *J. Geophys. Res. Atmos.* **119**: 529–545, doi: 10.1002/2013JD020890.

Ma ZG, Fu CB. 2003. Interannual characteristics of the surface hydrological variables over the arid and semi-arid areas of northern China. *Global Planet. Change* **37**: 189–200.

Ma ZG, Fu CB. 2005. Decadal variations of arid and semi-arid boundary in China. *Chinese J. Geophys.* **48**: 519–525 (in Chinese).

Marengo JA. 2006. On the hydrological cycle of the Amazon basin: a historical review and current state-of-the-art. *Rev. Bras. Meteorol.* **21**: 1–19.

Myoung B, Choi YS, Choi SJ, Park SK. 2012. Impact of vegetation on land-atmosphere coupling strength and its implication for desertification mitigation over East Asia. *J. Geophys. Res.* **117**: D12113, doi: 10.1029/2011JD017143.

Nakaegwa T. 2008. Reproducibility of the seasonal cycles of land-surface hydrological variables in Japanese 25-year Reanalysis. *Hydrol. Res. Lett.* **2**: 56–60.

Nicholson SE. 2000. Land surface processes and Sahel climate. *Rev. Geophys.* **38**: 117–139.

Onogi K, Tsutsui J, Koide H, Sakamoto M, Kobayashi S, Hatsushika H, Matsumoto T, Yamazaki N, Kamahori H, Takahashi K, Kadokura S, Wada K, Kato K, Oyama R, Ose T, Mannoji N, Taira R. 2007. The JRA-25 reanalysis. *J. Meteorol. Soc. Jpn.* **85**: 369–432.

Plaut G, Vautard R. 1994. Spells of low-frequency oscillations and weather regimes in the Northern Hemisphere. *J. Atmos. Sci.* **51**: 210–236.

Risi C, Noone D, Frankenberg C, Worden J. 2013. Role of continental recycling in intraseasonal variations of continental moisture as deduced from model simulations and water vapor isotopic measurements. *Water Resour. Res.* **49**: 4136–4156, doi: 10.1002/wrcr.20312.

Rowntree PR, Bolton JA. 1983. Simulation of the atmospheric response to soil moisture anomalies over Europe. *Q. J. R. Meteorol. Soc.* **109**: 501–526.

Salvucci GD, Saleem JA, Kaufmann R. 2002. Investigating soil moisture feedback on precipitation with tests of Granger causality. *Adv. Water Resour.* **25**: 1305–1312.

Santanello JA, Peters-Lidard CD, Kumar SV, Alonge C, Tao WK. 2009. A modeling and observational framework for diagnosing local land–atmosphere coupling on diurnal time scales. *J. Hydrometeorol.* **10**: 577–599, doi: 10.1175/2009JHM1066.1.

Schär C, Lüthi D, Beyerle U, Heise E. 1999. The soil–precipitation feedback: a process study with a regional climate model. *J. Clim.* **12**: 722–741.

Sellers PJ, Shuttleworth WJ, Dorman JL, Dalcher A, Roberts JM. 1989. Calibrating the Simple Biosphere model (SiB) for Amazonian tropical forest using field and remote sensing data: part I: average calibration with field data. *J. Appl. Meteorol.* **28**: 727–759.

Seneviratne SI, Lüthi D, Litschi M, Schär C. 2006. Land–atmosphere coupling and climate change in Europe. *Nature* **443**: 205–209, doi: 10.1038/nature05095.

Seneviratne SI, Corti T, Davin EL, Hirschi M, Jaeger EB, Lehner I, Orlowsky B, Teuling AJ. 2010. Investigating soil moisture–climate interactions in a changing climate: a review. *Earth Sci. Rev.* **99**: 125–161, doi: 10.1016/j.earscirev.2010.02.004.

Serafini YV. 1990. The time scale of land surface hydrology in response to initial soil moisture anomalies: a case study. *Tellus* **42A**: 390–400.

Shi YF, Shen YP, Li DL, Zhang GW, Ding YJ, Hu RJ, Kang ES. 2003. Discussion on the present climate change from warm-dry to warm-wet in Northwest China. *Quat. Sci.* **23**: 152–164 (in Chinese).

Taylor CM, Gounou A, Guichard F, Harris PP, Ellis RJ, Couvreux F, De Kauwe M. 2011. Frequency of Sahelian storm initiation enhanced over mesoscale soil-moisture patterns. *Nat. Geosci.* **4**: 430–433, doi: 10.1038/NGEO1173.

Taylor CM, de Jeu RAM, Guichard F, Harris PP, Dorigo WA. 2012. Afternoon rain more likely over drier soils. *Nature* **489**: 423–426, doi: 10.1038/nature11377.

Teuling AJ, Uijlenhoet R, Troch PA. 2005. On bimodality in warm season soil moisture observations. *Geophys. Res. Lett.* **32**: L13402, doi: 10.1029/2005GL023223.

Trenberth KE. 1999. Atmospheric moisture recycling: role of advection and local evaporation. *J. Clim.* **12**: 1368–1381.

Trenberth KE, Fasullo JT. 2013. Regional energy and water cycles: transports from ocean to land. *J. Clim.* **26**: 7837–7851, doi: 10.1175/JCLI-D-13-00008.1.

Trenberth KE, Dai A, Rasmussen RM, Parsons DB. 2003. The changing character of precipitation. *Bull. Am. Meteorol. Soc.* **84**: 1205–1217, doi: 10.1175/BAMS-84-9-1205.

Trenberth KE, Fasullo JT, Mackaro J. 2011. Atmospheric moisture transports from ocean to land and global energy flows in reanalyses. *J. Clim.* **24**: 4907–4924, doi: 10.1175/2011JCLI4171.1.

Tuinenburg OA, Hutjes RWA, Jacobs CMJ, Kabat P. 2011. Diagnosis of local land–atmosphere feedbacks in India. *J. Clim.* **24**: 251–266, doi: 10.1175/2010JCLI3779.1.

Vautard P, Yiou R, Ghil M. 1992. Singular-spectrum analysis: a toolkit for short, noisy chaotic signals. *Physica D: Nonlinear Phenomena* **58**: 95–126.

Vries PD, Döös K. 2001. Calculating Lagrangian trajectories using time-dependent velocity fields. *J. Atmos. Oceanic Technol.* **18**: 1092–1101.

Wang B, Ho L. 2002. Rainy season of the Asian–Pacific summer monsoon. *J. Clim.* **15**: 386–398.

Wang A, Zeng X. 2011. Sensitivities of terrestrial water cycle simulations to the variations of precipitation and air temperature in China. *J. Geophys. Res.* **116**: D02107, doi: 10.1029/2010JD014659.

Wang ZW, Zhai PM. 2003. Climate change in drought over northern China during 1950–2000. *Acta Geogr. Sin.* **58**: 61–68 (in Chinese).

Wang SW, Gong DY, Zhai PM. 2002. *Climate change in Western China, in Environmental Evolvement in Western China*. China Science, Press: Beijing (in Chinese).

Wang G, Kim Y, Wang D. 2007. Quantifying the strength of soil moisture–precipitation coupling and its sensitivity to changes in surface water budget. *J. Hydrometeorol.* **8**: 551–570, doi: 10.1175/JHM573.1.

Wei K, Wang L. 2013. Reexamination of the aridity conditions in arid Northwestern China for the last decade. *J. Clim.* **26**: 9594–9602, doi: 10.1175/JCLI-D-12-00605.1.

Westra D, Steeneveld GJ, Holtslag AAM. 2012. Some observational evidence for dry soils supporting enhanced relative humidity at the convective boundary layer top. *J. Hydrometeorol.* **13**: 1347–1358, doi: 10.1175/JHM-D-11-0136.1.

Yi L, Tao SY. 1997. Construction and analysis of a precipitation recycling model. *Adv. Water Sci.* **8**: 205–211 (in Chinese).

Zangvil A, Portis DH, Lamb PJ. 2001. Investigation of the large-scale atmospheric moisture field over the Midwestern United States in relation to summer precipitation. Part I: relationship between moisture budget components on different time scales. *J. Clim.* **14**: 582–597.

Zeng X, Barlage M, Castro C, Fling K. 2010. Comparison of land–precipitation coupling strength using observations and models. *J. Hydrometeorol.* **11**: 979–994, doi: 10.1175/2010JHM1226.1.

Zhang X, Sheng J, Shabbar A. 1998. Modes of interannual and interdecadal variability of Pacific SST. *J. Clim.* **11**: 2556–2569.

Zhang JY, Wang WC, Wei JF. 2008. Assessing land-atmosphere coupling using soil moisture from the global land data assimilation system and observational precipitation. *J. Geophys. Res.* **113**: D17119, doi: 10.1029/2008JD009807.

Zheng JY, Yin YH, Li BY. 2010. A new scheme for climate regionalization in China. *Acta Geogr. Sin.* **65**: 3–12 (in Chinese).

Zou XK, Zhai PM, Zhang Q. 2005. Variation in droughts over China: 1951–2003. *Geophys. Res. Lett.* **32**: L04707, doi: 10.1029/2004GL021853.

